Proceedings of the 9th World Congress on New Technologies (NewTech'23)
Brunel University, London, United Kingdom - August 09-11, 2023
Paper No. ICNFA 125
DOI: 10.11159/icnfa23.125

Molecular Dynamics Simulation as a Tool for Studying the Solvent in the Dye/TiO_2 Interaction in Natural Dye Sensitized Solar Cells

Arnold Huamán[1], María Quintana[1]
[1]National University of Engineering
Av. Túpac Amaru 210, Rímac 15333, Lima, Perú
ahuamanaguirre@gmail.com; mariavnac@gmail.ocom

Abstract **-** The present work focuses on studying the interaction between a natural dye, cyanidin-3-glucoside, and the TiO2 surface in sensitized solar cells. Molecular dynamics simulations based on the reactive force field ReaxFF were employed to investigate these interactions. Various solvent environments based on water and ethanol proportions were examined. The simulation results reveal that dye chemisorption always occurs, but with differences depending on the solvent used. A more favorable stability and Ti-O bond distance were observed in systems with solvent ratios of 1:1 and 1:3, suggesting improved dye loading under these conditions. Additionally, sensitized solar cells were prepared using the same solvents utilized in the simulation, and current-voltage and IPCE measurements were performed. It was found that cells prepared with the more stable solvent ratios exhibit higher photocurrent and efficiency. Overall, the results from the molecular simulation are in agreement with the experimental data, indicating its potential for predicting the optimal solvents to use in the preparation of natural dyes based on anthocyanins.

Keywords**:** Dye solar cells, cianidin-3-glucoside, molecular dynamics simulation, solvent environment, dye chemisorption.

1. Introduction

Natural dyes or photosensitizers derived from natural sources have received significant attention for use in dye-sensitized solar cells (DSSCs). Their easy extraction methods make them suitable candidates for replacing complex and expensive metal complexes or synthetic organic dyes [1]. However, there is still much unknown about the molecular interaction and anchoring mechanisms between these new natural dyes and the semiconductor electrode during sensitization. Furthermore, understanding the influence of the solvent environment would be advantageous for establishing an appropriate dye extraction process. This can be initially approached from a theoretical perspective using ab initio simulations [10], where molecular properties can be described using quantum mechanical (QM) methods. However, the high computational costs associated with QM limit its use to simulations with a relatively small number of atoms [2], [3].

A highly useful alternative is molecular dynamics (MD) simulations based on a reactive force field for calculating atomic interactions [4]. This method provides a precise description of the involved interactions (intermolecular, intramolecular, and molecule-surface) at desired temperatures. The ReaxFF reactive force field [5] is probably the most popular and has been used to simulate interactions at surface interfaces, successfully describing the chemisorption of the compounds involved [6], [7]. Additionally, the behaviour characteristics of certain solvents have been investigated [8], [9]. In the field of dye-sensitized solar cells, recent studies have examined the effects of organic dye aggregation [10] and the interactions between dye molecules and iodide ions in electrolytic species [11], shedding light on the dye regeneration mechanism.

In this work, we will study the interaction between the TiO_2 surface and a major compound found in purple corn, cyanidin-3-glucoside, under solvent environments with different proportions of water and ethanol. MD simulations will be performed using the ReaxFF reactive force field, allowing for a more realistic exploration in the spatial and temporal domains. Solar cells will be prepared to approximate the same conditions as in the simulation during sensitization. In addition, current-voltage (I-V) measurements will be conducted to assess the overall performance of the solar cell, and incident photon-to-current efficiency (IPCE) measurements will provide information on the dye's ability to convert solar light into electric current. This way, a correlation can be established between the solvent used and the final efficiency of the cell.

2. Experimental Procedure

2.1. Computational

The system based on the dye molecule cyanidin-3-glucoside (C3G) anchored to a TiO_2 nanoparticle and immersed in a water/ethanol mixture was simulated using LAMMPS. First, a 3D simulation box with dimensions of 6 x 5.5 x 4 nm was created, allowing space for three groups of atoms (solvent, C3G, and TiO2). The water and ethanol molecules were randomly placed within the simulation box in the necessary quantities to represent the solvent, taking into account the proportions used for experimental dye preparation. Next, the titanium dioxide atom network and the C3G molecule were separately equilibrated at ambient temperature and pressure. Both pre-equilibrated states were then imported into the same simulation box, with overlapping molecules removed and the new system re-equilibrated. The simulation of interatomic interactions was performed using the reactive force field ReaxFF for a duration of 7.5 ps, with a time integration step of 0.25 fs, under an isothermal-isobaric (NPT) ensemble at a temperature of 300 K.

2.2. Fabrication of Dye Solar Cells

The TiO_2 electrodes were prepared using the Doctor Blade method, where a paste of DSL 30NR-D titanium dioxide nanoparticles provided by Solaronix Company was deposited onto a square-shaped area (0.5 cm x 0.5 cm) of fluor-doped tin oxide (FTO). The film was then consolidated by thermal treatment at 450°C for 45 minutes. On the other hand, the counter electrode was prepared from a precursor solution of 5 mM hexachloroplatinic acid (IV) hexahydrate in ethanol. The solution was deposited onto FTO by spin coating and subsequently subjected to thermal treatment at 450°C for 15 minutes.

The natural dye was obtained through the following procedure. Purple corn was husked and dehydrated at 80°C for 24 hours. Then, the husk was scraped to obtain flakes from the surface layer, which were subsequently ground into a fine powder using a mortar and pestle. 100 mg of the obtained product was diluted in 50 mL of water, ethanol, and a mixture of both in proportions of 1:3, 1:1, and 3:1. After one hour of agitation at room temperature, the resulting solution was centrifuged and filtered multiple times to remove solid residues. Subsequently, the TiO2 films were immersed in the solution for sensitization for 24 hours.

The electrolyte used in this work consists of a 0.6 M 4-tert-butylpyridine, 0.05 M I2, and 0.10 M LiI dissolved in acetonitrile. The mixture was stirred for approximately three hours, resulting in a standard electrolyte based on the iodide/triiodide redox couple. The working electrode and counter electrode were sealed using small amounts of Surlyn® (60 mm), a special thermoplastic sealant, which was applied around the active area of the electrode, leaving two small opposing openings for the electrolyte to enter.

3. Results and Discussions

3.1. Molecular Dynamics Simulation

The semiconductor network of titanium dioxide was constructed in its anatase phase in the tetragonal system with space group I41/a m d, having lattice parameters of a = 373 Å and c = 9.37 Å, extending it to 60 unit cells (Fig. 1a). After equilibrating the system, a structure with a more spheroidal shape was obtained. Several oxygen atoms and some titanium atoms were lost as can be observed in Fig. 1b. This is consistent with theoretical and experimental evidence of oxygen vacancies in anatase, which contribute to increased surface activity [12]. Before incorporating the other groups of atoms into the same simulation box, the detached atoms were removed to only consider the resulting central structure. Fig. 2 presents the equilibrated structure of the C3G group with the initial relative positions of its atoms that will be placed close to the TiO2 group.

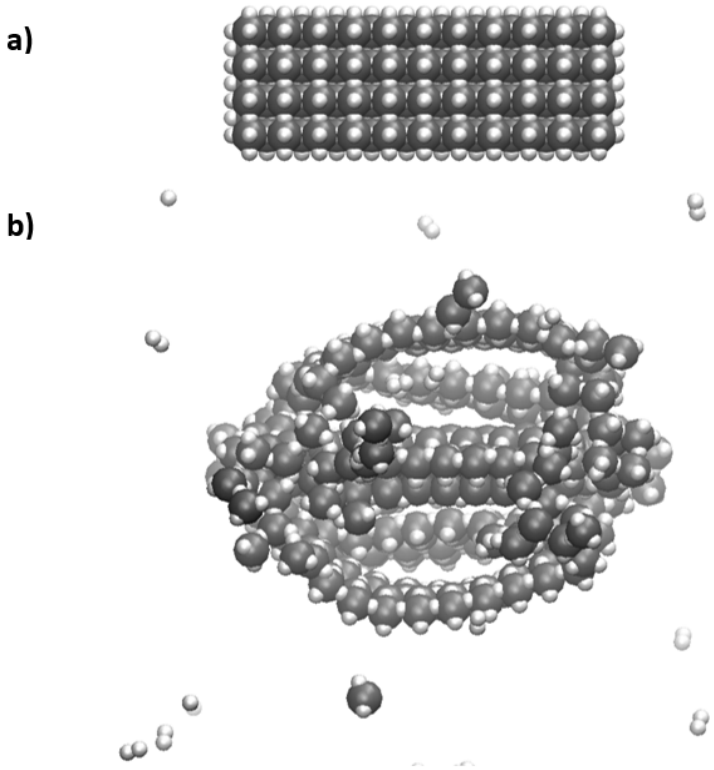

Fig. 1: a) Theoretical construction of the TiO_2 network in its anatase phase in the [0 1 0] orientation. b) Final positions of the Ti (grey) and O (white) atoms after balancing the system.

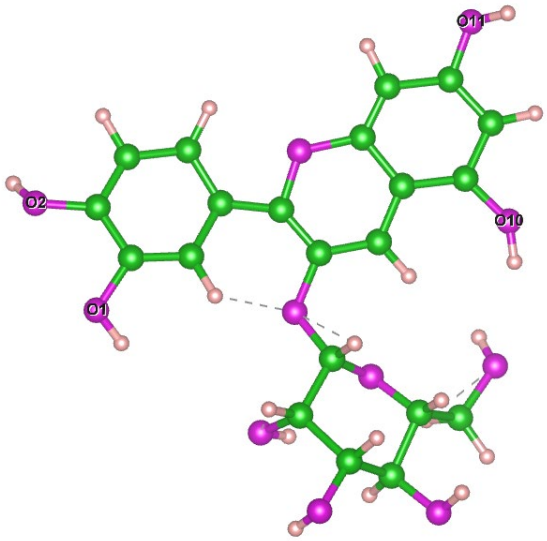

Fig. 2: Representative structure of cyanidin-3-glucoside after being equilibrated. C: Green. O: purple. H: Pink.

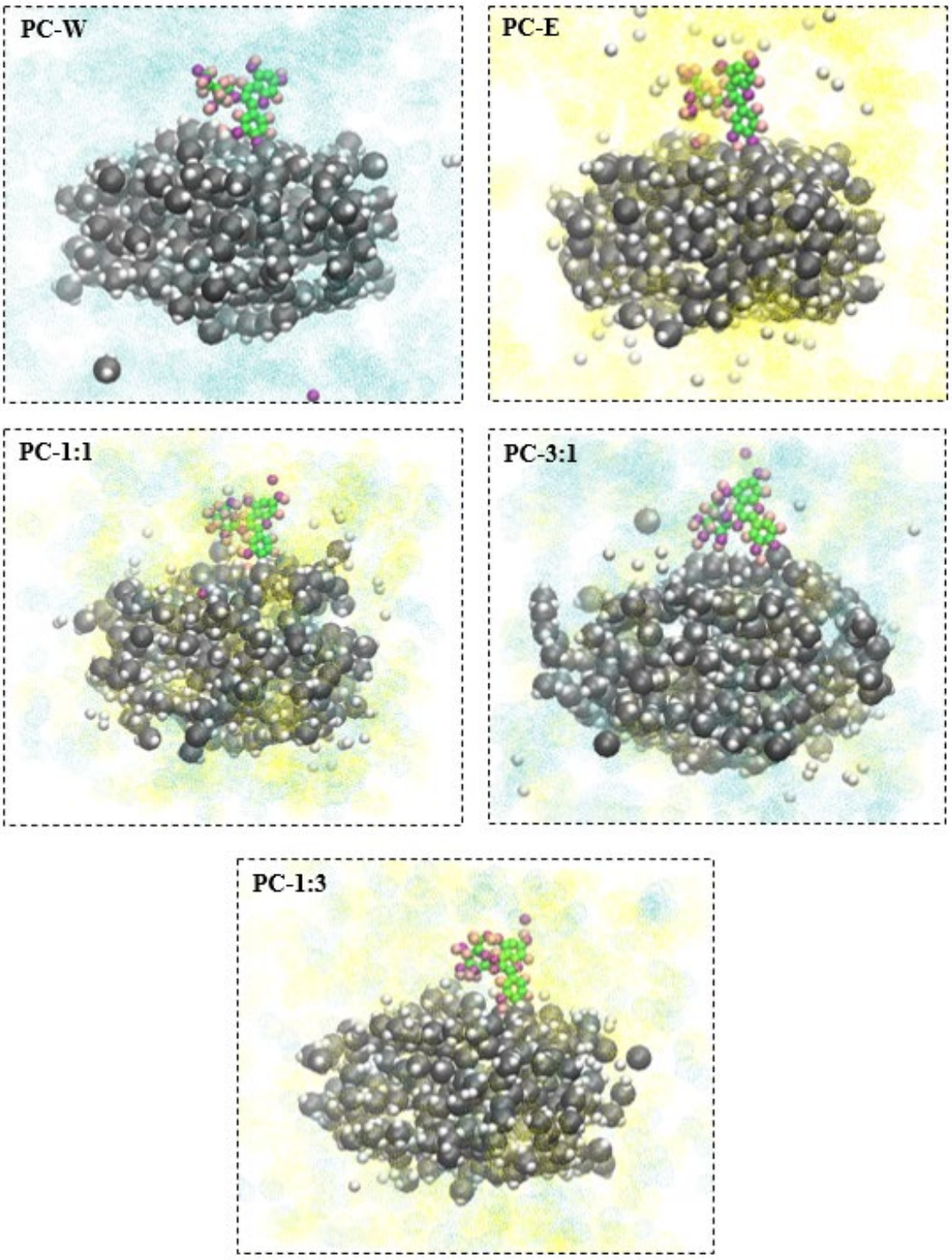

Fig. 3: Snapshots of C3G chemisorption events on TiO_2 in water (PC-W), ethanol (PC-E), 50% water with 50% ethanol (PC-1:1), 75% water with 25% ethanol (PC -3:1), and 25% water with 75% stanol (PC-1:3) during MD simulations.

For all cases, the simulation demonstrated that chemisorption was always effective, although it varied depending on the scenario. As shown in Figure 3, in the PC-W, PC-E, and PC-3:1 case, a bond formed between the oxygen at the O2 site of C3G and the nearest Ti atom. In the PC-1:1 and PC-1:3 cases, it was observed that C3G lost the oxygen from the O2 site, and the free carbon formed a bond with the oxygen of the nearest TiO2. In all cases, coordination always took place through the same hydroxyl group of C3G. On the other hand, titanium dioxide continued to lose oxygen, with a visibly higher loss observed in the ethanol case, and some titanium atoms also became detached. Similarly, C3G always lost at least one oxygen atom from the glucoside portion, which tended to remain in the solvent, and hydrogen atoms ended up on the surface of titanium dioxide.

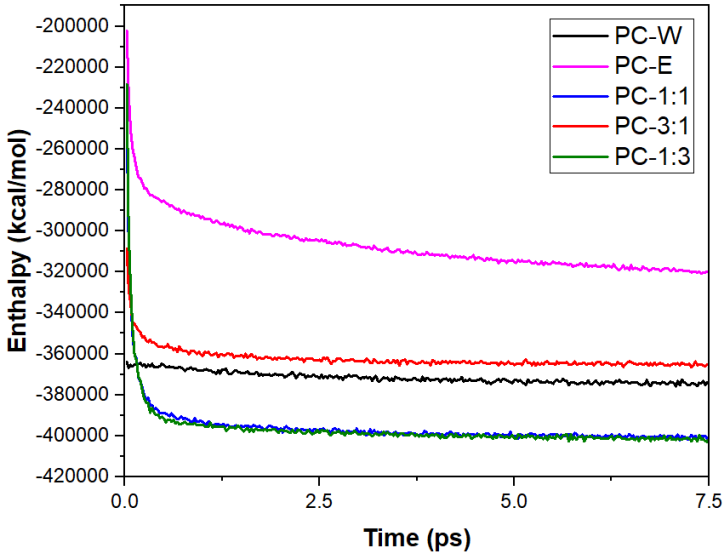

Fig. 4: Total enthalpy vs. time for the simulations of the TiO_2/C3G systems.

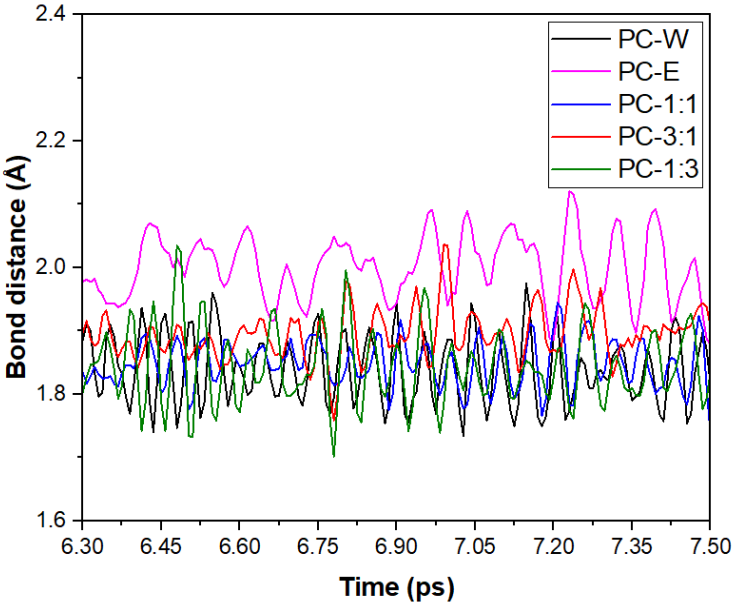

Fig. 5: Ti-O bond distance formed between the anchoring oxygen of the C3G and the closest titanium of the TiO_2 particle between the simulation times 6.3 and 7.5 ps.

In order to ensure that the models are well equilibrated during the NPT simulation, data on the total enthalpy over time were collected for all solvated systems, and the graph is presented in Figure 4. It can be observed from the curves that the enthalpy reaches a nearly constant value with relatively small fluctuations, indicating that the simulation times were sufficient to reach equilibrium states. Based on the graph, we can conclude that in thermodynamic terms, the PC-1:1 and PC-1:3 systems are the most stable, favoring the anchoring reactions of C3G, which is important for achieving better dye loading.

Figure 5 shows the variation of the Ti-O bond distance responsible for the chemisorption of the dye molecule in each case. The last picoseconds of simulation are shown, which is when the systems have reached equilibrium. The distances range from 1.7 Å to 2.1 Å, which fall within the expected range for this type of bond [13]. However, it can be observed that in the case of the ethanol solvent, the bond distance is greater than in the other cases. This indicates the lower stability of the bond, which is consistent with the higher enthalpy shown in the graph in Figure 4.

3.2. Solar Cell Characterization

Figure 6 shows the current-voltage (I-V) curves of the cells prepared with different solvent ratios and the corresponding incident photon-to-electron conversion efficiency (IPCE) curves, which are consistent with the obtained photocurrent intensities. Table 1 presents the values of power conversion efficiency (PCE), open-circuit voltage (VOC), short-circuit current density (JSC), and fill factor (FF) of the solar cells. It can be observed that the highest photocurrent (0.881 mA/cm2) and fill factor (0.587) are achieved with the PC-1:3 solvent. When comparing pure solvents, water shows the best results. However, it is clear that the combined solvents were more successful.

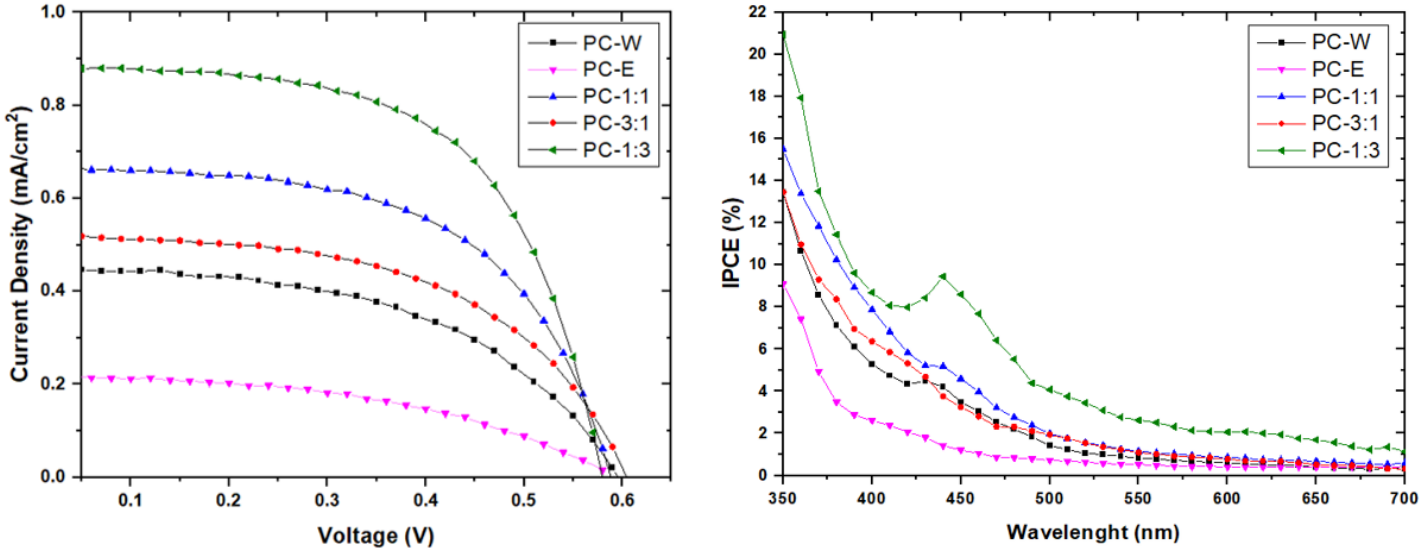

Fig. 6: Current-voltage (left) and IPCE (right) curves of the solar cells fabricated with the films sensitized with different concentrations of solvents.

Table 1: Main parameters of the cells fabricated with the different proportions of water and ethanol.

Solvent	PCE (%)	V_{OC} (V)	J_{SC} (mA/cm^2)	FF
PC-W	0.130±0.008	0.595±0.011	0.456±0.034	0.498±0.028
PC-E	0.057±0.013	0.593±0.012	0.199±0.053	0.479±0.012
PC-1:1	0.225±0.022	0.58±0.012	0.664±0.037	0.583±0.025
PC-3:1	0.163±0.016	0.602±0.013	0.497±0.048	0.546±0.008
PC-1:3	0.303±0.009	0.587±0.009	0.881±0.010	0.587±0.018

The obtained photocurrents are closely related to the MD simulation. We observed that the PC-1:1 and PC-1:3 systems, which were the most stable according to the enthalpy graph, achieved the highest efficiencies. Similarly, the PC-E system, which was the least stable, obtained the lowest efficiency. Naturally, if the chemisorption is more favored in a particular solvent, a higher dye loading will be achieved, leading to a better utilization of solar light for electron donation in the titanium dioxide network [14], resulting in improved photocurrents.

4. Conclusion

MD simulations demonstrated that chemisorption between the dye and titanium dioxide was effective for all studied systems, albeit with variations depending on the solvent used. The PC-1:1 and PC-1:3 systems exhibited higher stability and favored the dye anchoring reaction, which is crucial for achieving a better dye loading in the solar cell. Characterization of the solar cells sensitized with different solvents revealed that these cases achieved the highest power conversion efficiencies, correlating with the MD simulation results. Therefore, MD simulation can aid in predicting the optimal solvent options to optimize the photocurrents obtained in anthocyanin-based dye-sensitized solar cells, such as purple corn.

Acknowledgements

This work would not have been possible without the support and financing of CONCYTEC / PROCIENCIA Program through project 058-2021.

References

[1] F. Kabir, S. N. Sakib, and N. Matin, “Stability study of natural green dye based DSSC,” Optik (Stuttg), vol. 181, pp. 458–464, Mar. 2019, doi: 10.1016/J.IJLEO.2018.12.077.

[2] R. Tatti et al., “Synthesis of single layer graphene on Cu (111) by C60 supersonic molecular beam epitaxy,” RSC Adv, vol. 6, no. 44, pp. 37982–37993, 2016, doi: 10.1039/c6ra02274j.

[3] R. Palacios-Rivera et al., “Surface specificity and mechanistic pathway of de-fluorination of C60F48on coinage metals,” Nanoscale Adv, vol. 2, no. 10, pp. 4529–4538, Oct. 2020, doi: 10.1039/d0na00513d.

[4] S. Irle, G. Zheng, Z. Wang, and K. Morokuma, “The C60 formation puzzle ‘solved’: QM/MD simulations reveal the shrinking hot giant road of the dynamic fullerene self-assembly mechanism,” Journal of Physical Chemistry B, vol. 110, no. 30, pp. 14531–14545, Aug. 2006, doi: 10.1021/jp061173z.

[5] T. P. Senftle et al., “The ReaxFF reactive force-field: development, applications and future directions,” npj Computational Materials 2016 2:1, vol. 2, no. 1, pp. 1–14, Mar. 2016, doi: 10.1038/npjcompumats.2015.11.

[6] B. Saha, A. S. Patra, A. K. Mukherjee, and I. Paul, “Interaction and thermal stability of carboxymethyl cellulose on α-Fe2O3(001) surface: ReaxFF molecular dynamics simulations study,” J Mol Graph Model, vol. 102, Jan. 2021, doi: 10.1016/j.jmgm.2020.107787.

[7] J. Yeon, S. C. Chowdhury, and J. W. Gillespie, “Hydroxylation and water-surface interaction for S-glass and silica glass using ReaxFF based molecular dynamics simulations,” Appl Surf Sci, vol. 608, p. 155078, Jan. 2023, doi: 10.1016/J.APSUSC.2022.155078.

[8] S. Y. Kim, A. C. T. van Duin, and J. D. Kubicki, “Molecular dynamics simulations of the interactions between TiO2 nanoparticles and water with Na+ and Cl-, methanol, and formic acid using a reactive force field,” J Mater Res, vol. 28, no. 3, pp. 513–520, Feb. 2013, doi: 10.1557/jmr.2012.367.

[9] S. Rasouli, M. R. Moghbeli, and S. J. Nikkhah, “A comprehensive molecular dynamics study of a single polystyrene chain in a good solvent,” Current Applied Physics, vol. 18, no. 1, pp. 68–78, Jan. 2018, doi: 10.1016/j.cap.2017.10.010.

[10] W. Zhang, Y. Zhang, H. Su, X. Zhu, L. Wang, and J. Zhang, “The effects of dye aggregation on the performance of organic dyes in dye-sensitized solar cells: From static model to molecular dynamics simulation,” J Lumin, vol. 205, pp. 7–13, Jan. 2019, doi: 10.1016/j.jlumin.2018.08.084.

[11] L. He, Y. Guo, and L. Kloo, “An Ab Initio Molecular Dynamics Study of the Mechanism and Rate of Dye Regeneration by Iodide Ions in Dye-Sensitized Solar Cells,” ACS Sustain Chem Eng, vol. 10, no. 6, pp. 2224–2233, Feb. 2022, doi: 10.1021/ACSSUSCHEMENG.1C08101/ASSET/IMAGES/LARGE/SC1C08101_0018.JPEG.

[12] M. A. Ha and A. N. Alexandrova, “Oxygen Vacancies of Anatase (101): Extreme Sensitivity to the Density Functional Theory Method,” J Chem Theory Comput, vol. 12, no. 6, pp. 2889–2895, Jun. 2016, doi: 10.1021/acs.jctc.6b00095.
[13] C. I. Oprea, P. Panait, Z. M. Essam, R. M. Abd El-Aal, and M. A. Gîrțu, “Photoexcitation processes in oligomethine cyanine dyes for dye-sensitized solar cells—synthesis and computational study,” Nanomaterials, vol. 10, no. 4, Apr. 2020, doi: 10.3390/nano10040662.
[14] M.-E. Yeoh and K.-Y. Chan, “Recent advances in photo-anode for dye-sensitized solar cells: a review,” Int J Energy Res, vol. 41, no. 15, pp. 2446–2467, Dec. 2017, doi: https://doi.org/10.1002/er.3764.